Effect of an oblique magnetic field on the superparamagnetic relaxation time

W. T. Coffey*
Department of Electronic and Electrical Engineering, Trinity College, Dublin 2, Ireland

D. S. F. Crothers
Department of Applied Mathematics and Theoretical Physics, The Queen's University of Belfast, Belfast BT7 1NN, Northern Ireland

J. L. Dormann
Laboratoire de Magnétisme et d'Optique de l'Université de Versailles, URA 1531, Bâtiment Fermat, 45 avenue des États-Unis, 78035 Versailles Cedex, France

L. J. Geoghegan
Department of Electronic and Electrical Engineering, Trinity College, Dublin 2, Ireland

Yu. P. Kalmykov
Institute of Radio Engineering and Electronics, Vvedenski Square 1, Fryazino, Moscow Region, 141120, Russia

J. T. Waldron
School of Computer Applications, Dublin City University, Glasnevin, Dublin 9, Ireland

A. W. Wickstead
Department of Pure Mathematics, The Queen's University of Belfast, Belfast BT7 1NN, Northern Ireland
(Received 27 December 1994; revised manuscript received 20 July 1995)

The effect of a constant magnetic field, applied at an angle ψ to the easy axis of magnetization, on the Néel relaxation time τ of a single domain ferromagnetic particle (with uniaxial anisotropy) is studied by calculating the lowest nonvanishing eigenvalue λ_1 (the escape rate) of the appropriate Fokker-Planck equation using matrix methods. The effect is investigated by plotting λ_1 versus the anisotropy parameter α for various values of ψ, and the ratio $h=\xi/2\alpha$, where ξ is the external field parameter and λ_1 versus ψ for various h values (for rotation of the magnetization vector **M** both in a plane and in three dimensions). If **M** rotates in a plane the curve of λ_1 versus ψ is symmetric about $\psi=\pi/4$ in the range $0<\psi<\pi/2$ and significant decrease in τ with increasing ψ is predicted for large ξ and α. The maximum decrease in τ occurs at $\psi=\pi/4$ whereupon τ increases again to the $\psi=0$ value at $\psi=\pi/2$. For rotation of **M** in three dimensions, the curve of λ_1 versus ψ $(0<\psi<\pi)$ is symmetric about $\psi=\pi/2$. Thus the maximum decrease in τ again occurs at $\psi=\pi/4$ with maximum increase to a value exceeding that at $\psi=0$ (i.e., with the field applied along the polar axis with that axis taken as the easy axis), at $\psi=\pi/2$ (field applied along the equator), the $\psi=0$ value being again attained at $\psi=\pi$. The results are shown to be consistent with the behavior predicted by the Kramers theory of the rate of escape of particles over potential barriers. This theory when applied to the potential barriers for the equatorial orientation of the field for rotation in three dimensions yields a simple approximate formula for the escape rate which is in reasonable agreement with the exact λ_1 calculated from the Fokker-Planck equation. Pfeiffer's approximate formula for the barrier height as a function of α [H. Pfeiffer, Phys. Status Solidi **122**, 377 (1990)] is shown to be in reasonable agreement with our results.

I. INTRODUCTION

The effect of an external constant magnetic field **H** on the longitudinal relaxation time τ of fine single-domain ferromagnetic particles having simple uniaxial anisotropy may be studied[1,2] by calculating the smallest nonvanishing eigenvalue λ_1 (the escape rate) of the Fokker-Planck equation. This equation governs the time evolution of the density of magnetic moment orientations $W(\vartheta,\phi,t)$ on a sphere of radius M_s (the mean magnetization of a nonrelaxing particle), the orientation of the magnetic moment **M** being specified by the spherical polar coordinates (ϑ,ϕ). For simple uniaxial anisotropy the ratio of the potential energy vV to the thermal energy kT is

$$\frac{vV}{kT} = -\alpha(\mathbf{e}\cdot\mathbf{n})^2 - \xi(\mathbf{e}\cdot\mathbf{h}). \tag{1}$$

In Eq. (1), v is the volume of the single-domain particle; $\alpha=Kv/kT$ is the anisotropy barrier height parameter; K is the anisotropy constant; $\xi=vM_sH/kT$ is the external field parameter; **e**, **n**, and **h** are unit vectors in the direction of the magnetization vector **M**, the internal anisotropy (or easy) axis, and **H**, respectively.

The Néel relaxation time, which is the time required for the magnetization to surmount the potential barrier given by Eq. (1), is related[1,2] to λ_1 by the equation

$$\tau \cong \frac{\tau_N}{\lambda_1}, \tag{2}$$

where τ_N is the diffusional relaxation time given by[1]

$$\tau_N=\frac{\beta\eta M_s^2(1+a^2)}{2a^2}, \tag{3}$$

γ is the gyromagnetic ratio, η is a phenomenological damping constant,[1] with units such that

$$a=\eta\gamma M_s$$

and

$$\beta=\frac{v}{kT}.$$

In the notation of Ref. 1

$$2\tau_N=\frac{1}{k'}.$$

The original calculations of λ_1 by Brown[1] and Aharoni[2] for rotation of **M** in three dimensions were carried out under the assumption that **H** is parallel to the easy axis **n**. This restriction allowed them to retain the axial symmetry associated with the zero external field solution[1-3] thus simplifying the solution of the Fokker-Planck equation as only the zonal harmonics are involved. In particular, Aharoni[2] showed by a numerical solution of the Fokker-Planck equation that Brown's[1] asymptotic formula for λ_1 namely,

$$\lambda_1\cong\pi^{-1/2}\alpha^{3/2}(1-h^2)\{(1+h)\exp[-\alpha(1+h)^2]+(1-h)\exp[-\alpha(1-h)^2]\}, \tag{4}$$

derived using the Kramers escape rate theory,[4-6] provides a good approximation to λ_1 for $h\leqslant 0.4$ and $\alpha\geqslant 2$. If h tends to zero Eq. (4) becomes

$$\lambda_1\cong 2\pi^{-1/2}\alpha^{3/2}e^{-\alpha} \tag{5}$$

yielding the well-known formula[1]

$$\frac{\tau}{\tau_N}\cong\frac{\sqrt{\pi}}{2}\alpha^{-3/2}e^{\alpha},\quad \alpha\geqslant 2,$$

so that the Néel relaxation time is

$$\tau\cong\beta\eta\frac{M_s^2(1+a^2)}{a^2}\frac{\sqrt{\pi}}{4}\alpha^{-3/2}e^{\alpha}.$$

In this paper we report the behavior of λ_1 when the assumption that $\mathbf{H}\|\mathbf{n}$ is abandoned, as in practice the easy axis is in a random position.[7] The calculation proceeds by reducing the problem of solving the Fokker-Planck equations pertaining to the rotation of **M** both in three dimensions[3] (3D) and in a plane[8] to the solution of sets of differential-recurrence relations. These arise by expanding the solution for rotation of **M** in 3D as a series of normalized spherical harmonics and for rotation of **M** in a plane as a series of circular functions. The recurrence relations for rotation in a plane depend on the *single* integer variable p. On the other hand, for rotation in 3D, apart from the special case of axial symmetry where the field is parallel to the easy axis, *two* integers l and m will be involved. Such recurrence relations may in turn be arranged as an infinite set of simultaneous linear differential equations of the first order. The lowest nonvanishing root of the characteristic equation of such a set, when truncated at the number of equations necessary to achieve convergence, then yields λ_1.

We also report the behavior of λ_1 for rotation of **M** in a plane because this restriction which confines the recurrence relations to a single variable considerably reduces the numerical difficulties in computing λ_1 for large ξ and α (the range of parameter values, which is of most interest) without sacrificing most of the important qualitative features associated with the fact that **H** is no longer parallel to **n**.

II. DIFFERENTIAL-RECURRENCE RELATIONS FOR ROTATION IN THREE DIMENSIONS

In order to discuss rotation of **M** in 3D we may suppose without significant loss of generality that the spherical polar coordinates of **e**, **n**, and **h** are (ϑ,ϕ), (0,0), and $(\psi,0)$ that is the field is in the $(x\text{-}z)$ plane or applied along a line of longitude. Thus the potential of Eq. (1) is of the form (it is most useful for the purpose of calculations involving the spherical harmonics to take the anisotropy axis as the polar axis)

$$\beta V(\vartheta,\phi)=\alpha\sin^2\vartheta-\xi\cos\psi\cos\vartheta-\xi\sin\psi\sin\vartheta\cos\phi,\qquad 0\leqslant\vartheta\leqslant\pi,\quad 0\leqslant\phi\leqslant 2\pi, \tag{6}$$

with

$$V(\phi\pm 2m\pi)=V(\phi),$$

$$m=0,1,2,3,\ldots,\infty.$$

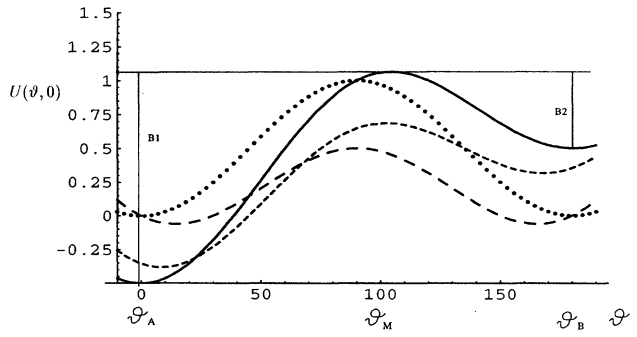

FIG. 1. Variation with polar angle ϑ of the potential function $U(\vartheta,0)=\alpha^{-1}\beta V(\vartheta,0)$ in the x-z plane for various values of ψ the angle between the external field and the easy axis: dots are $h=0$, solid line $\psi=0$, small dashed line $\psi=\pi/4$, large dashed line $\psi=\pi/2$ (the last three curves are drawn for $h=0.25$). The bistable character of the potential is preserved in all cases. B_1 and B_2 are the potential barriers shown for $\psi=0$. ϑ_A and ϑ_B are the angular positions of the minima, ϑ_m is the angular position of the maximum corresponding to a *saddle point* of $V(\vartheta,\phi)$ and occurs near the equator. ϑ_A corresponds to a deep potential minimum in the $\phi=0$, longitude near the north pole, ϑ_B to a shallow minimum in the $\phi=0$ longitude near the south pole. If the potential is extended to the unit circle $0\leqslant\vartheta\leqslant 2\pi$, there is a stationary point ϑ_C which corresponds to a simple maximum of $V(\vartheta,\phi)$ over the whole unit sphere and so is of no interest in the present problem.

For the purpose of the discussion of λ_1 we are interested in the behavior of this potential in the x-z plane, $\phi=0$ where $V(\vartheta,\phi)=V(\vartheta,0)$ and in the range $0\leqslant\vartheta\leqslant\pi$ since $\phi=0$ contains a saddle point of $V(\vartheta,\phi)$. The variation of $V(\vartheta,0)$ is shown as a function of ϑ in Fig. 1 for $h=0.25$. It is apparent if h is less than a certain critical value h_c which varies (see Sec. IV) from 0.5 for $\psi=\pi/4$ to 1 for $\psi=0$, $\pi/2$, that $V(\vartheta,0)$ has two minima separated by a maximum [which corresponds to a saddle point of $V(\vartheta,\phi)$] and two potential barriers B_1 and B_2. If $h>h_c$ the two minima structure of the potential disappears and $V(\vartheta,0)$ has a simple maximum. For $h=h_c$ the second minimum becomes a point of inflexion. The two minima have in general different energies so that the energy barriers are not equal and only part of the magnetic moment relaxes. On account of the inequality of the barriers the chief contribution to λ_1 for large α and $h<h_c$ will be that due to the magnetic moment surmounting the lower barrier B_2.

The Fokker-Planck equation derived by Brown[1] for the density of orientations of $\mathbf{M}$ is [with $V=V(\vartheta,\phi)$, and Ω the rotational operator $\mathbf{e}\times\nabla$]

$$2\tau_N\frac{\partial W}{\partial t}=\Omega^2 W+\frac{\beta}{\sin\vartheta}\frac{\partial}{\partial\vartheta}\left(\sin\vartheta\frac{\partial V}{\partial\vartheta}W-\frac{1}{a}\frac{\partial V}{\partial\phi}W\right)+\frac{\beta}{\sin\vartheta}\frac{\partial}{\partial\phi}\left(\frac{1}{\sin\vartheta}\frac{\partial V}{\partial\phi}W+\frac{1}{a}\frac{\partial V}{\partial\vartheta}W\right). \quad (7)$$

Ω^2 is the angular part of the Laplacian, that is

$$\Omega^2=\frac{1}{\sin\vartheta}\frac{\partial}{\partial\vartheta}\left(\sin\vartheta\frac{\partial}{\partial\vartheta}\right)+\frac{1}{\sin^2\vartheta}\frac{\partial^2}{\partial\phi^2}.$$

The terms in a^{-1} in Eq. (7) are precessional or gyromagnetic terms which give rise to ferromagnetic resonance at high frequencies. If the potential is axially symmetric so that $V=V(\vartheta)$ as holds if $\mathbf{H}\|\mathbf{n}$ then these terms do not contribute to the longitudinal relaxation time. On the other hand, if $\mathbf{H}$ is not parallel to $\mathbf{n}$ as in the present problem these terms may strictly only be neglected if the phenomenological damping coefficient η is such that

$$\eta\gamma M_s\gg 1,$$

while in practice $\eta\gamma M_s$ is of order 0.2–1. However, the main contribution of these terms is to the high-frequency response, thus we shall suppose that they may be ignored so reducing the numerical problems associated with the calculation of λ_1 from the set of differential-recurrence relations arising from Eq. (7).

In order to calculate λ_1 we seek the aftereffect solution of the Fokker-Planck equation following a small change $\Delta\mathbf{H}$ in $\mathbf{H}$. Thus at times $t\leqslant 0$ the system was at equilibrium and the probability density W was given by the Boltzmann distribution

$$W(\vartheta,\phi,0)=W^0_{\xi+\xi_1}(\vartheta,\phi)=\frac{\exp[-\alpha\sin^2\vartheta+(\xi+\xi_1)(\cos\vartheta\cos\psi+\sin\vartheta\cos\phi\sin\psi)]}{\int_0^{2\pi}\int_0^{\pi}\exp[-\alpha\sin^2\vartheta+(\xi+\xi_1)(\cos\vartheta\cos\psi+\sin\vartheta\cos\phi\sin\psi)]\sin\vartheta d\vartheta d\phi}$$
$$\cong W^0_\xi(\vartheta,\phi)\{1+\xi_1\cos\psi[\cos\vartheta-\langle\cos\vartheta\rangle_0]+\xi_1\sin\psi[\sin\vartheta\cos\phi-\langle\sin\vartheta\cos d\phi\rangle_0]\}. \quad (8)$$

The statistical average

$$\langle\ \rangle_0=\frac{\int_0^{2\pi}\int_0^{\pi}(\ )W^0_\xi(\vartheta,\phi)\sin\vartheta d\vartheta d\phi}{\int_0^{2\pi}\int_0^{\pi}W^0_\xi(\vartheta,\phi)\sin\vartheta d\vartheta d\phi}$$

is to be evaluated in the absence of the perturbation

$$\xi_1=\frac{vM_s\Delta H}{kT}.$$

This condition is denoted by the subscript zero on the angular brackets. As $t\to\infty$, $W(\vartheta,\phi,t)$ tends to the equilibrium distribution $W^0_\xi(\vartheta,\phi)$. The aftereffect solution is sought in the form of the Laplace series

$$W(\vartheta,\phi,t)=\sum_{l=0}^{\infty}\sum_{m=-l}^{l}a_{l,m}(t)Y_{l,m}(\vartheta,\phi) \quad (9)$$

and $a_{l,-m}=(-1)a^*_{lm}$ since W is real. The form of the solution chosen ensures that W and its derivatives are finite at the poles $\vartheta=0$, π of the sphere and are periodic in ϕ.

The $Y_{l,m}(\vartheta,\phi)$ are the normalized spherical harmonics[9] defined by

$$Y_{l,m}(\vartheta,\phi)=N_{l,m}P^m_l(\cos\vartheta)e^{im\phi},\quad -l\leqslant m\leqslant l,$$
$$Y_{l,m}=(-1)^m Y^*_{l,-m} \quad (10)$$

where the asterisk denotes the complex conjugate. The P^m_l are the associated Legendre functions and the normalization constants are

$$N_{l,m}=(-1)^m\sqrt{\frac{(2l+1)(l-m)!}{4\pi(l+m)!}}.$$

The $P^m_l(x)$ are defined[9] by ($x=\cos\vartheta$)

$$P^m_l(x)=\frac{(1-x^2)^{m/2}}{2^l l!}\frac{d^{l+m}}{dx^{l+m}}(x^2-1)^l$$

which allows us[9] to define $P^m_l(x)$ for negative m as

$$P^{-m}_l(x)=(-1)^m\frac{(l-m)!}{(l+m)!}P^m_l(x)$$

and $P_l(x)$ is the Legendre polynomial of order l. This symmetry relation is very important as it avoids the necessity of solving differential-recurrence relations for negative m. The

potential of Eq. (6) may be expressed in terms of the normalized spherical harmonics as follows:

$$\beta V=\alpha\left(\frac{2}{3}-\sqrt{\frac{16\pi}{45}}\,Y_{2,0}\right)-\xi\cos\psi\sqrt{\frac{4\pi}{3}}\,Y_{1,0}+\xi\sin\psi\sqrt{\frac{2\pi}{3}}\,(Y_{1,1}-Y_{1,-1}). \tag{11}$$

We also note that (neglecting the gyromagnetic terms) the Fokker-Planck equation may be written in the form which most readily allows us to exploit the properties of the $Y_{l,m}$ namely

$$2\tau_N\frac{\partial W}{\partial t}=\Omega^2W+\frac{\beta}{2}\,(W\Omega^2V-V\Omega^2W+\Omega^2VW) \tag{12}$$

and

$$\Omega^2Y_{l,m}(\vartheta,\phi)=-l(l+1)Y_{l,m}(\vartheta,\phi).$$

Equation (12) follows from the identity

$$\nabla\cdot(W\nabla V)=\tfrac{1}{2}[W\nabla^2V+\nabla^2(WV)-V\nabla^2W]$$

with Ω replacing ∇.

On substituting Eq. (9) into Eq. (12) and using the orthogonality properties of the $Y_{l,m}$, namely[9]

$$\int_{\phi=0}^{2\pi}\int_{\vartheta=0}^{\pi}Y_{p,q}Y_{l,m}^{*}\sin\vartheta\,d\vartheta\,d\phi=\delta_{p,l}\delta_{q,m}$$

together with the recurrence relations[9] for $Y_{1,1}Y_{l,m}$, $Y_{1,0}Y_{l,m}$, $Y_{1,-1}Y_{l,m}$ we obtain the following set of differential-recurrence relations for the expansion coefficients $a_{l,m}$ of the Laplace series of Eq. (9):

$$\begin{aligned}2\tau_N\dot{a}_{l,m}+l(l+1)a_{l,m}=2\alpha\Bigg(&\frac{(l+1)}{(2l-1)}\sqrt{\frac{(l-m-1)(l+m)(l-m)(l+m)}{(2l-3)(2l+1)}}\,a_{l-2,m}+\frac{l(l+1)-3m^2}{(2l-1)(2l+3)}\,a_{l,m}\\&-\frac{l}{2l+3}\sqrt{\frac{(l-m+2)(l+m+2)(l-m+1)(l+m+1)}{(2l+1)(2l+5)}}\,a_{l+2,m}\Bigg)\\&+\xi\cos\psi\Bigg((l+1)\sqrt{\frac{(l-m)(l+m)}{(2l-1)(2l+1)}}\,a_{l-1,m}-l\sqrt{\frac{(l-m+1)(l+m+1)}{(2l+1)(2l+3)}}\,a_{l+1,m}\Bigg)\\&+\frac{1}{2}\,\xi\sin\psi\Bigg((l+1)\sqrt{\frac{(l-m-1)(l-m)}{(2l-1)(2l+1)}}\,a_{l-1,m+1}+l\sqrt{\frac{(l+m+2)(l+m+1)}{(2l+1)(2l+3)}}\,a_{l+1,m+1}\\&-(l+1)\sqrt{\frac{(l+m-1)(l+m)}{(2l-1)(2l+1)}}\,a_{l-1,m-1}-l\sqrt{\frac{(l-m+2)(l-m+1)}{(2l+1)(2l+3)}}\,a_{l+1,m-1}\Bigg).\end{aligned} \tag{13}$$

These in turn may be written as a set of differential-recurrence relations for the decay (aftereffect) functions $c_{l,m}(t)$ which are the averages of the real solid harmonics. We have

$$c_{l,m}(t)=\langle P_l^m(\cos\vartheta)\cos m\phi\rangle-\langle P_l^m(\cos\vartheta)\cos m\phi\rangle_0,$$

where the symbol $\langle\,\rangle_0$ indicates that the averages are to be calculated in the absence of the perturbation $\Delta\mathbf{H}$ and

$$\langle P_l^m(\cos\vartheta)\cos m\phi\rangle=\frac{a_{l,m}+(-1)^ma_{l,-m}}{2a_{0,0}N_{l,m}}=\frac{\mathrm{Re}\,\{a_{l,m}\}}{a_{0,0}N_{l,m}},$$

where the $c_{l,m}(t)$ satisfy

$$\begin{aligned}2\tau_N\dot{c}_{l,m}+l(l+1)c_{l,m}=2\alpha\Bigg[&\frac{(l+1)(l+m-1)(l+m)}{(2l-1)(2l+1)}\,c_{l-2,m}+\frac{l(l+1)-3m^2}{(2l-1)(2l+3)}\,c_{l,m}-\frac{l(l-m+2)(l-m+1)}{(2l+1)(2l+3)}\,c_{l+2,m}\Bigg]\\&+\frac{\xi\cos\psi}{2l+1}\,[(l+1)(l+m)c_{l-1,m}-l(l-m+1)c_{l+1,m}]\\&+\frac{\xi\sin\psi}{2(2l+1)}\,[(l+1)(l+m-1)(l+m)c_{l-1,m-1}+l(l-m+2)(l-m+1)c_{l+1,m-1}\\&-(l+1)c_{l-1,m+1}-lc_{l+1,m+1}],\end{aligned} \tag{14}$$

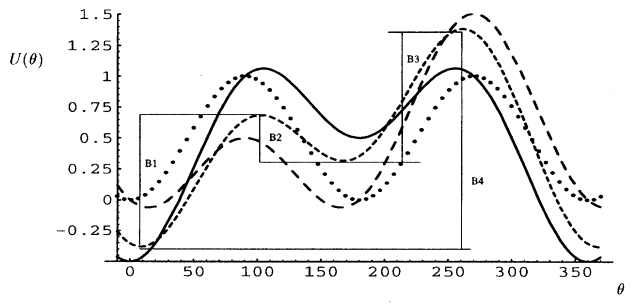

FIG. 2. Variation with plane polar angle θ of the potential function $U(\theta)$ for rotation in a plane: dots are $h=0$, solid line $\psi=0$, small dashed line $\psi=\pi/4$, large dashed line $\psi=\pi/2$ (the last three curves are drawn for $h=0.25$). The metastable character of one cycle of the potential is preserved in all cases.

which is a nine-term differential-recurrence relation for the $c_{l,m}$. The terms prefixed by α are those which arise from simple uniaxial anisotropy. The $\xi\cos\psi$ and $\xi\sin\psi$ terms arise from the longitudinal and transverse components of **H**. In particular the decay function of the magnetization is

$$b(t)=nM_s[\cos\psi c_{l,0}(t)+\sin\psi c_{l,1}(t)], \tag{15}$$

where n is the number of particles per unit volume. If the gyromagnetic effects had been included, terms in $\langle P_l^m(\cos\vartheta)\sin m\phi\rangle$ and their l,m differences would appear in our Eq. (14) so increasing the numerical complexity of the calculations required to determine λ_1 because of the increase in the number of terms in the differential-recurrence relation.

III. DIFFERENTIAL-RECURRENCE RELATIONS FOR ROTATION IN A PLANE

Equation (7) pertains to rotation of the magnetization vector **M** in 3D. If **M** is constrained to rotate in the X-Y plane, the corresponding Fokker-Planck equation is[8] of the form

$$\tau_N\frac{\partial F}{\partial t}=\beta\frac{\partial}{\partial\theta}\left(F\frac{\partial V}{\partial\theta}\right)+\frac{\partial^2 F}{\partial\theta^2}, \tag{16}$$

where $F(\theta,t)$ is now the probability density of orientations of **M** on a circle of radius M_s with θ the *plane* polar angle specifying the orientation of **M** and the potential energy function is (Fig. 2)

$$\beta V(\theta)=\alpha\sin^2\theta-\xi\cos(\theta-\psi),$$

$$0\leq\theta\leq 2\pi \tag{17}$$

with V defined elsewhere by periodicity. Equation (17) differs as shown in Fig. 2 from $V(\vartheta,0)$ because the range of θ is $[0,2\pi]$ so that $V(\theta)$ for $h<h_c$ has *two* maxima and *two* minima in one cycle. We note that τ_N in Eq. (16) *et seq.* is twice the value given by Eq. (3) as is appropriate for rotation in a plane. The aftereffect solution may be found as a Fourier series

$$F(\theta,t)=\sum_{p=-\infty}^{p=\infty}a_p(t)e^{-ip\theta} \tag{18}$$

which ensures that $F(\theta,t)$ and its derivatives are periodic in θ, with

$$a_{-p}=a_p^*(t)$$

since F is real and

$$\langle e^{ip\theta}\rangle=\frac{a_{-p}(t)}{a_0} \tag{19}$$

which leads to the differential-recurrence relation for the aftereffect functions $c_p(t)$

$$\frac{d}{dt}c_p+\frac{p^2}{\tau_N}c_p=\frac{\xi p}{2\tau_N}[e^{-i\psi}c_{p-1}-e^{i\psi}c_{p+1}]+\frac{\alpha p}{2\tau_N}[c_{p-2}-c_{p+2}], \tag{20}$$

where

$$c_p(t)=\langle e^{ip\theta}\rangle-\langle e^{ip\theta}\rangle_0=f_p(t)+ig_p(t).$$

Equation (20) may be conveniently arranged as a set of simultaneous linear differential-recurrence relations for the sine and cosine averages $f_p(t)$ and $g_p(t)$ namely

$$\frac{df_p}{dt}+\frac{p^2 f_p}{\tau_N}=\frac{\alpha p}{2\tau_N}(f_{p-2}-f_{p+2})+\frac{\xi p}{2\tau_N}[\cos\psi(f_{p-1}-f_{p+1})-\sin\psi(g_{p-1}+g_{p+1})],$$

$$\frac{dg_p}{dt}+\frac{p^2}{\tau_N}g_p=\frac{\alpha p}{2\tau_N}(g_{p-2}-g_{p+2})+\frac{\xi p}{2\tau_N}[\sin\psi(f_{p-1}+f_{p+1})+\cos\psi(g_{p-1}-g_{p+1})], \tag{21}$$

so avoiding the need to solve Eq. (20) for negative p because

$$f_{-p}=f_p,$$

$$g_{-p}=-g_p.$$

The decay function of the magnetization is

$$b(t)=nM_s[\cos\psi f_p(t)+\sin\psi g_p(t)]. \tag{22}$$

We emphasize that Eq. (20) is a five-term differential-recurrence relation in the *single* variable p rather than the nine-term one of the $c_{l,m}$ in the *pair* of variables, (l,m), where the range of m is $2l+1$ so posing a much easier computational task while reproducing many qualitative features of the three-dimensional problem. In order to discuss the calculation of λ_1 from Eq. (14) or (21), we must now describe[10] the behavior of the potential energy Eq. (6) or (17) as a function of the applied field **H**. In particular,[8] we note for $h=0$ the analogous result to Eq. (5)

$$\lambda_1=4\pi^{-1}\alpha e^{-\alpha},\quad \alpha\geq 2,$$

yielding $\tau/\tau_N\cong(\pi/4)(e^\alpha/\alpha)$.

IV. BEHAVIOR OF THE POTENTIAL ENERGY

We consider the detailed calculation of the behavior of the potential energy as a function of the applied field **H** for Eq. (6) (rotation in 3D) as the calculation for rotation in a plane is essentially similar. We first rewrite Eq. (6) in the form ($0 \leqslant \vartheta \leqslant \pi$, $0 \leqslant \phi \leqslant 2\pi$)

$$U(\vartheta,\phi)=\frac{\beta V(\vartheta,\phi)}{\alpha}=\sin^2\vartheta-2h(\cos\psi\cos\vartheta + \sin\psi\sin\vartheta\cos\phi), \tag{23}$$

where

$$h=\frac{\xi}{2\alpha}. \tag{24}$$

The stationary points occur for $\phi=0$ and $\phi=\pi$. The stationary point for $\phi=\pi$ corresponds to a *maximum* of Eq. (23) and so is of no interest. The stationary points for $\phi=0$ correspond to a *saddle point* of Eq. (23) at ϑ_m and minima at ϑ_A and ϑ_B for $h<h_c$. The saddle point is generally in the equatorial region, while ϑ_A and ϑ_B lie in the north and south polar regions, respectively.

The two equilibrium directions of the magnetization and their associated polar angles ϑ_A, ϑ_B lie[11] in the x-z plane ($\phi=0$) and are determined by the conditions for a minimum of $U(\vartheta,0)$ namely[10,13]

$$\frac{\partial U}{\partial\vartheta}=0, \quad \frac{\partial^2 U}{\partial\vartheta^2}>0. \tag{25}$$

The position of the saddle point follows from the conditions for a maximum of $U(\vartheta,0)$, namely,

$$\frac{\partial U}{\partial\vartheta}=0, \quad \frac{\partial^2 U}{\partial\vartheta^2}<0 \tag{26}$$

and the critical value of the ratio of field to barrier height parameter h_c at which the potential loses its bistable character follows from the condition for a double root (point of inflexion) of $U(\vartheta,0)$, namely,

$$\frac{\partial U}{\partial\vartheta}=\frac{\partial^2 U}{\partial\vartheta^2}=0. \tag{27}$$

Equation (27) now yields

$$\frac{1}{2}\sin 2\vartheta=-h_c\sin(\vartheta-\psi), \tag{28}$$

$$\cos 2\vartheta=-h_c\cos(\vartheta-\psi) \tag{29}$$

that is

$$\tan 2\vartheta=2\tan(\vartheta-\psi) \tag{30}$$

or with

$$\tan\vartheta=t$$

$$t^3=-\tan\psi \tag{31}$$

the only real root of which is [the range of ϑ is $(0,\pi)$]

$$\tan\vartheta=-(\tan\psi)^{1/3} \tag{32}$$

so that with Eq. (28)

$$h_c=-\frac{\sin\vartheta\cos\vartheta}{\sin\vartheta\cos\psi-\cos\vartheta\sin\psi}=\frac{1}{\cos\psi\left[1+\left(\frac{\sin\psi}{\cos\psi}\right)^{2/3}\right]^{3/2}}, \tag{33}$$

$$h_c^2=\frac{1}{(\cos^{2/3}\psi+\sin^{2/3}\psi)^3}. \tag{34}$$

Equation (33) may also be written in terms of $\tan\psi$ as

$$h_c=\frac{(1+\tan^2\psi)^{1/2}}{[1+(\tan\psi)^{2/3}]^{3/2}}. \tag{35}$$

The Stoner-Wohlfahrt calculation[11–13] we have just outlined, leads to the equation that determines the value of h at which the potential barrier vanishes as a function of ψ, namely,

$$(1-h_c^2)^3-\tfrac{27}{4}h_c^4\sin^2 2\psi=0. \tag{36}$$

The corresponding value of $\tan\psi$ satisfies the biquadratic equation

$$\tan^4\psi+\tan^2\psi\left[2-\frac{27h_c^4}{(1-h_c^2)^3}\right]+1=0. \tag{37}$$

It should be noted that in the calculations of Stoner and Wohlfahrt[13] and that of Pfeiffer[11,12] the external field axis is taken as the polar axis. Thus in their calculations the quantities $(\vartheta-\psi)$ and ϑ in Eq. (30) are interchanged. In their coordinate system, Eq. (30) would read

$$\tan 2(\vartheta-\psi)=2\tan\vartheta. \tag{38}$$

Our choice of angles has the merit that it is much easier to derive the set of differential-recurrence relations for the $c_{l,m}$ using such a coordinate system. Equation (33) also holds for planar rotation, where we recall that in this case the polar angle ϑ is replaced by the plane polar angle θ with $0 \leqslant \theta \leqslant 2\pi$.

It is evident[13] (referring to rotation in 3D) from Eq. (36) (from the requirement for real solutions) that $|h_c|$ lies in the range $1/2 \leqslant |h_c| \leqslant 1$, the value $|h_c|=1$ occurring for $\psi=0$ or $\pi/2$ and $|h_c|=1/2$ for $\psi=\pi/4$, hence one would expect that the greatest increase in the value of λ_1 (lowering of the Néel time) would occur at $\psi=\pi/4, 3\pi/4$. The corresponding critical values of ϑ are, from Eqs. (31) and (37), $3\pi/4$ and $\pi/4$.

In general for $\psi \neq 0$ it is not particularly simple to evaluate the various derivatives and hence the barrier heights B_1 and B_2 as a function of h and ψ from the Stoner-Wohlfahrt analysis given above. However, for particular values of ψ, e.g., $\psi=0$, we easily find that

$$B_1=\alpha(1+h)^2, \tag{39}$$

$$B_2=\alpha(1-h)^2, \tag{40}$$

and the potential has the *asymmetric* bistable form shown in Fig. 1. For $\psi=\pi/2$, on the other hand, the barriers B_1 and B_2 coincide so that

$$B_1=B_2=\alpha(1-h)^2 \tag{41}$$

and the potential assumes a *symmetric* bistable form reminiscent of that for $h=0$ (see Fig. 1). For other values of ψ, Pfeiffer[11,12] who studied the present problem in the discrete orientation approximation, has shown by a numerical analysis of the Stoner-Wohlfahrt theory, that the lower barrier height B_2 which determines almost entirely the nature of the relaxation process is given by the approximate expression

$$B_2=\alpha\left[1-\frac{h}{h_c(\psi)}\right]^{0.86+1.14h_c(\psi)}, \tag{42}$$

where h_c is to be calculated from Eq. (34). In general for rotation of **M** in space the potential retains its *asymmetric bistable* form for $0<h<h_c$ and $\psi\neq\pi/2$. Furthermore, for $\psi=\pi/4$, the potential barrier B_2 is a minimum with $h_c=0.5$.

Analogous remarks apply to the potential of Eq. (17) pertaining to rotation of **M** in a plane, making due allowance for the fact that the potential is now periodic in θ with period 2π (Fig. 2) so that *four* potential barriers B_1,B_2,B_3,B_4 will exist in one cycle of the potential. Hence for $\psi=0$, and $0<h<1$ one cycle of the potential has a symmetric *metastable* form each of the low barriers coincide, and have height $\alpha(1-h)^2$ while the height of the high barriers is $\alpha(1+h)^2$. Thus the escape routes at $\theta=0$ and 2π are severely curtailed. For $\psi=\pi/4$, B_2 is a minimum with $h_c=0.5$ just as in 3D rotation, and a cycle of the potential has an asymmetric metastable form. For $\psi=\pi/2$, the asymmetrical metastable form is retained, the escape route at $\theta=0$ being severely curtailed by the high left-hand barrier $\alpha(1+h)^2$. However, at $\theta=2\pi$ particles may easily enter from the right by crossing the barrier $\alpha(1-h)^2$. Thus unlike rotation in 3D the relaxation time for $\psi=0$ is the same as for $\psi=\pi/2$ if **M** is constrained to rotate in a plane. It should be noted taking account of the periodic character of the potential that the $\psi=\pi/2$ potential is just the negative of the $\psi=0$ one. We remark that the metastable character of the relaxation process for rotation in a plane is preserved in the limit $h\to 0$ as the potential executes two oscillations in $0<\theta<2\pi$ so that there are now four equal potential barriers.

V. APPROXIMATE EXPRESSIONS FOR $\lambda_1(\psi)$

The foregoing discussion of the behavior of the potential barriers as a function of ψ suggests that the Kramers approach used by Brown to derive a formula for $\lambda_1(\psi)$ for $\mathbf{H}\|\mathbf{n}$, namely [Eq. (4)],

$$\lambda_1\cong\pi^{-1/2}\alpha^{3/2}(1-h^2)\{(1+h)\exp[-\alpha(1+h)^2] +(1-h)\exp[-\alpha(1-h)^2]\}, \tag{43}$$

$h\leq 0.4$, $\alpha\geq 2$ may be used with suitable modification to treat the orientation $\psi=\pi/2$, i.e., $\mathbf{H}\perp\mathbf{n}$. We note in passing that the leading term in Eq. (43) is often ignored[2] so that

$$\lambda_1(0)\cong\pi^{-1/2}\alpha^{3/2}(1-h^2)\{(1-h)\exp[-\alpha(1-h)^2]\}. \tag{44}$$

This corresponds to ignoring the rate of escape of particles over the high barrier B_1 in Fig. 1.

Equation (43) is derived from Brown's general formula for the reciprocal p_1 of the longest time constant for an axially symmetric potential which has minima at $\vartheta=0$, and $\vartheta=\pi$ and a maximum at $\vartheta=\vartheta_m$, namely,

$$p_1=\nu_{12}+\nu_{21},$$

where

$$\nu_{ij}=\frac{1}{2\tau_N}\beta V_i''\left[-\beta\frac{V''(\vartheta_m)}{2\pi}\right]^{1/2}\sin\vartheta_m e^{-\beta[V(\vartheta_m)-V_i]}$$

$$(i=1,\ j=2\quad\text{or}\quad i=2,\ j=1), \tag{45}$$

where

$$V_1=V''(0),\quad V_2=V''(\pi).$$

The lowest eigenvalue λ_1 in our notation is then

$$\lambda_1=\tau_n(\nu_{12}+\nu_{21}).$$

Equation (43) then follows from Eq. (45), the quantities $V_i'',V''(\vartheta_m)$, $B_i=\beta[V(\vartheta_m)-V_i]$ being evaluated from Eq. (23) with $\psi=0$, $\phi=0$.

Now for a field applied perpendicular to the easy axis, i.e., along the equator the potential is a *symmetric bistable* one where the barrier heights B_1 and B_2 are coincident and equal so that

$$B_1=B_2=\alpha(1-h)^2. \tag{46}$$

This suggests at a cursory glance that the barrier crossing process could be described by Eq. (5) with α replaced by Eq. (46). Thus

$$\lambda_1\left(\frac{\pi}{2}\right)\cong 2\pi^{-1/2}\alpha^{3/2}(1-h)^3\exp[-\alpha(1-h)^2],$$

$$\alpha(1-h)^2\geq 2. \tag{47}$$

Such an approach is however incorrect in this case since the fundamental formula Eq. (45) on which Eq. (47) is based must be modified as the form of the potential function $\beta V(\vartheta,0)$ for $\psi=\pi/2$ is

$$\beta V(\vartheta,0)=\alpha(\sin^2\vartheta-2h\sin\vartheta). \tag{48}$$

This function, unlike the case $\psi=0$ which has minima at $\vartheta=0$ and $\vartheta=\pi$ and a maximum at $\vartheta_m=\cos^{-1}h$, has minima at $\vartheta=\vartheta_A=\sin^{-1}h$ and $\vartheta_B=\pi-\sin^{-1}h$ and a central maximum at $\vartheta_m=\pi/2$. In order to apply Brown's approach correctly, we consider a potential which has minima at ϑ_A and $(\pi-\vartheta_A)$ and a maximum at ϑ_m. This allows one to calculate an asymptotic formula for $\lambda_1(\pi/2)$ and may very easily be extended to all ψ values as we demonstrate at the end of this section. We first recall that Eq. (7) has the form of the continuity equation

$$\frac{\partial W}{\partial t}+\operatorname{div}\mathbf{J}=0, \tag{49}$$

where **J** is a surface current density of representative points on the unit sphere with components

$$J_\vartheta=\frac{-\beta}{2\tau_N}\left[\left(\frac{\partial V}{\partial\vartheta}-\frac{1}{a\sin\vartheta}\frac{\partial V}{\partial\phi}\right)W\right]-\frac{1}{2\tau_N}\frac{\partial W}{\partial\vartheta}, \tag{50}$$

$$J_\phi = -\frac{\beta}{2\tau_N}\left[\left(\frac{1}{a}\frac{\partial V}{\partial \vartheta}+\frac{1}{\sin\vartheta}\frac{\partial V}{\partial \phi}\right)W\right]-\frac{1}{2\tau_N}\frac{1}{\sin\vartheta}\frac{\partial W}{\partial \phi}. \tag{51}$$

We shall now, following the Kramers transition state theory[1,4,14] assume that most of the representative points on the unit sphere are concentrated at the energy minima of $V(\vartheta,0)$ where they are in thermal equilibrium so that W has the Maxwell-Boltzmann distribution. Thus[14] only a minute fraction of the representative points is outside the energy minima so allowing a *small* diffusion current between them which is a manifestation of the nonequilibrium conditions. We also assume that the system is *quasistationary* in that between the energy minima

$$\frac{\partial W}{\partial t}=0. \tag{52}$$

Hence by the continuity equation (49)

$$\operatorname{div}\mathbf{J}=0. \tag{53}$$

In accordance with the above remarks almost all the particles in $0<\vartheta<\vartheta_1<\vartheta_m$ have orientations between $(\vartheta_A-\varepsilon)$ and $(\vartheta_A+\varepsilon)$ in a small range ε about ϑ_A and almost all the particles in $\vartheta_m<\vartheta_2<\vartheta<\pi$ have orientations in a small range $\pi-(\vartheta_A+\varepsilon)$, $\pi-(\vartheta_A-\varepsilon)$ about $(\pi-\vartheta_A)$. Thus in the region $(0,\vartheta_1)$ we have

$$W(\vartheta)=W(\vartheta_A)e^{-\beta[V(\vartheta)-V(\vartheta_A)]} \tag{54}$$

and in the region (ϑ_2,π) we have

$$W(\vartheta)=W(\pi-\vartheta_A)e^{-\beta[V(\vartheta)-V(\pi-\vartheta_A)]}. \tag{55}$$

If following Brown[1] we normalize $\int W d\Omega$ to be the total number n of particles (where $d\Omega$ is an element of solid angle) the number n_1 in $0<\vartheta<\vartheta_1$ is

$$n_1=2\pi W(\vartheta_A)e^{\beta V(\vartheta_A)}\int_{\nu_A-\varepsilon}^{\nu_A+\varepsilon}e^{-\beta V(\vartheta)}\sin\vartheta d\vartheta$$

so that

$$n_1=2\pi W(\vartheta_A)e^{\beta V(\vartheta_A)}I_1, \tag{56}$$

where

$$I_1=\int_{\vartheta_A+\varepsilon}^{\vartheta_A+\varepsilon}e^{-\beta V(\vartheta)}\sin\vartheta d\vartheta \tag{57}$$

and in $\vartheta_2<\vartheta<\pi$

$$n_2=2\pi W(\pi-\vartheta_A)e^{\beta V(\pi-\vartheta_A)}I_2, \tag{58}$$

where

$$I_2=\int_{\pi-(\vartheta_A+\varepsilon)}^{\pi-(\vartheta_A-\varepsilon)}e^{-\beta V(\vartheta)}\sin\vartheta d\vartheta. \tag{59}$$

Because of the rapid decrease of the exponential factors in Eqs. (57) and (59) with distance from the minima of V at ϑ_A and $(\pi-\vartheta_A)$, we may in I_1 replace $V(\vartheta,0)$ by its Taylor series about $\vartheta=\vartheta_A$ truncated at the $(\vartheta-\vartheta_A)^2$ term (the $\vartheta-\vartheta_A$ term vanishes); replace sin ϑ by sin ϑ_A and the upper and lower limits by ∞ and $-\infty$, hence

$$I_1\cong\sin\vartheta_A e^{-\beta V(\vartheta_A)}\int_{-\infty}^{\infty}e^{-\beta[(\vartheta-\vartheta_A)^2/2]V''(\vartheta_A)}d\vartheta$$

$$=\sin\vartheta_A e^{-\beta V(\vartheta_A)}\sqrt{\frac{2\pi}{\beta V''(\vartheta_A)}}. \tag{60}$$

In like manner

$$I_2\cong\sin\vartheta_A e^{-\beta V(\pi-\vartheta_A)}\sqrt{\frac{2\pi}{\beta V''(\pi-\vartheta_A)}}. \tag{61}$$

In the region $\vartheta_1<\vartheta<\vartheta_2$ in which the maximum ϑ_m lies we saw that W is very small but still sufficient to maintain a small net flow of representative points from the overpopulated towards the underpopulated minimum. If we assume that the gyromagnetic terms in Eqs. (50) and (51) may be neglected then the flow may be approximated sufficiently[1] by a zero divergence current density so that the total current in the (x,z) plane is

$$I=2\pi\sin\vartheta J_\vartheta. \tag{62}$$

Hence Eq. (50) becomes

$$\frac{\partial W}{\partial\vartheta}+\beta\frac{\partial V}{\partial\vartheta}W=-\frac{2\tau_N I_m I}{2\pi\sin\vartheta}. \tag{63}$$

Now following Brown we may multiply Eq. (63) by the integrating factor $e^{\beta V}$ and integrate from ϑ_1 to ϑ_2 to get

$$We^{\beta V}\Big|_{\vartheta_1}^{\vartheta_2}=\frac{-2\tau_N I_m I}{2\pi}, \tag{64}$$

where

$$I_m=\int_{\vartheta_1}^{\vartheta_2}\frac{e^{\beta V}d\vartheta}{\sin\vartheta}. \tag{65}$$

Here we replace V by its Taylor series about the maximum $\vartheta=\vartheta_m$ and truncate at the $(\vartheta-\vartheta_m)^2$ term; replace sin ϑ by sin ϑ_m; and integrate from $-\infty$ to ∞ to get, as in Ref. 1,

$$I_m=\left[\frac{2\pi}{-\beta V''(\vartheta_m)}\right]^{1/2}\frac{e^{\beta V_m}}{\sin\vartheta_m}. \tag{66}$$

Now following the argument of Ref. 1 the left-hand member of Eq. (64) is from Eqs. (54) and (55),

$$W(\pi-\vartheta_A)e^{\beta V(\pi-\vartheta_A)}-W(\vartheta_A)e^{\beta V(\vartheta_A)}=\frac{1}{2\pi}\left(\frac{n_2}{I_2}-\frac{n_1}{I_1}\right). \tag{67}$$

Equation (63) relates Eq. (67) to the current I from the region $(0,\vartheta_1)$ to the region (ϑ_2,π). However, following the reasoning of Ref. 1 practically all the representative points are in these regions (they are concentrated at ϑ_A and $\pi-\vartheta_A$). Hence

$$I=\dot{n}_1=-\dot{n}_2=-\frac{1}{2\tau_N I_m}\left(\frac{n_2}{I_2}-\frac{n_1}{I_1}\right). \tag{68}$$

This is of the form

$$\dot{n}_1=-\dot{n}_2=n_2\nu_{21}-n\nu_{12} \tag{69}$$

with

$$\nu_{ij}=\frac{1}{2\tau_N I_m I_i}, \quad (i=1,\ j=2 \quad \text{or} \quad i=2,\ j=1). \tag{70}$$

Hence

$$\lambda_1=\tau_N(\nu_{12}+\nu_{21}),$$

which on substituting for I_m, I_1, and I_2 becomes

$$\lambda_1\left(\frac{\pi}{2}\right)=\frac{1}{4\pi}\frac{\sin\vartheta_m}{\sin\vartheta_A}[-\beta V''(\vartheta_m)]^{1/2} \times\{[\beta V''(\vartheta_A)]^{1/2}e^{-\beta[V(\vartheta_m)-V(\vartheta_A)]} +[\beta V''(\pi-\vartheta_A)]^{1/2}e^{-\beta[V(\vartheta_m)-V(\pi-\vartheta_A)]}\}. \tag{71}$$

Equation (71) is an asymptotic formula for $\lambda_1(\pi/2)$ for a symmetric bistable potential which has minima at ϑ_A and $\vartheta_A-\pi$ and a maximum at $\vartheta_m=\pi/2$ lying in $\vartheta_A<\vartheta<(\pi-\vartheta_A)$. It has a different form to Eq. (45) which assumes that the minima are at $\vartheta=0$ and $\vartheta=\pi$. We saw that for $\psi\neq 0$, or $\pi/2$ that the potential $V(\vartheta,0)$ has an asymmetric bistable form. All the arguments leading to Eq. (71) also apply for an arbitrary ψ. We merely have to recall that in general the minima will be at $\vartheta_A>0$, $\vartheta_B<\pi$ separated by a maximum at ϑ_m and that the escape rates ν_{12} and ν_{21} are no longer equal. Equation (71) is then modified to

$$\lambda_1(\psi)=\frac{1}{4\pi}\sin\vartheta_m[-\beta V''(\vartheta_m)]^{1/2} \times\left\{\frac{\beta V''(\vartheta_A)^{1/2}}{\sin\vartheta_A}e^{-\beta[V(\vartheta_m)-V(\vartheta_A)]} +\frac{[\beta V''(\vartheta_B)]^{1/2}}{\sin\vartheta_B}e^{-\beta[V(\vartheta_m)-V(\vartheta_B)]}\right\}, \tag{72}$$

where the transition points ϑ_A, ϑ_B, and ϑ_m are to be determined by solving

$$\beta V'(\vartheta,0)=0.$$

The particular cases $\lambda_1(\pi/2)$, $\lambda_1(\pi/4)$ are compared with the numerical solution in Sec. VII.

VI. PROCEDURE FOR THE NUMERICAL CALCULATION OF $\lambda_1(\psi)$

We shall first plot (following the procedure of Aharoni[2] for the axially symmetric potential) λ_1 as a function of h for given ψ. In order to accomplish this, we arrange the hierarchy of differential-recurrence relations in the matrix form

$$\dot{\mathbf{X}}=\mathbf{A}\mathbf{X}, \tag{73}$$

where

$$\mathbf{X}=\begin{pmatrix} c_{1,0} \\ c_{1,1} \\ c_{2,0} \\ \vdots \end{pmatrix} \tag{74}$$

and $\mathbf{A}$ is the system matrix the elements of which are determined by Eq. (14). The column vector $\mathbf{X}$ does not include $c_{l,m}$ for negative m because they are calculated using the symmetry relation deduced from the definition of $P_l^{-m}(x)$

$$c_{l,-m}=(-1)^m\frac{(l-m)!}{(l+m)!}c_{l,m}. \tag{75}$$

$\lambda_1$is then the smallest nonvanishing root of the characteristic equation

$$\det(\lambda\mathbf{I}-\mathbf{A})=0. \tag{76}$$

The same considerations hold for the hierarchy of Eq. (21), with the difference that it is convenient to work with the real and imaginary parts $f_p(t)$ and $g_p(t)$ of $c_p(t)$ so that

$$\mathbf{X}=\begin{pmatrix} f_1 \\ g_1 \\ f_2 \\ g_2 \\ \vdots \end{pmatrix} \tag{77}$$

with

$$f_{-p}=f_p,$$

$$g_{-p}=-g_p. \tag{78}$$

The calculation of λ_1 for rotation in a plane, i.e., $\mathbf{X}$ given by Eq. (77) is quite straightforward using *Mathematica*'s built-in Eigenvalues function. Satisfactory convergence was found for $\alpha=10$ with an 80×80 matrix $\mathbf{A}$ in all cases. If α is increased to 20 convergence is achieved by taking a 200×200 matrix. This is not true, however, for rotation in space where the system of differential-recurrence relations contains the numbers l,m and their various differences. Initially we again attempted to compute the smallest eigenvalue of the matrix using *Mathematica*'s built-in Eigenvalues function. Although this produced results for values of α up to about 5, beyond that the smallest eigenvalue that was produced failed to converge even when matrix sizes of up to 1300×1300 were used. Estimates of the size of numbers involved in the calculation suggested that loss of precision in floating point calculations was to blame rather than lack of convergence in the strictly mathematical problem. As partial confirmation that this was indeed the problem, we continued the calculations for a relatively small value of α beyond the 150×150 matrices which gave apparent convergence of the eigenvalue and found that by 400×400 the eigenvalue returned was not even real. Similar difficulties appear to have been encountered by Eisenstein and Aharoni[14,15] in their numerical calculations of λ_1 for cubic anisotropy potentials. This again effectively involves the calculation of inverses of the matrices generated by the differential-recurrence relations for the real solid harmonic averages $c_{l,m}$. Thus the range of validity of their calculation was severely curtailed.[16]

As an alternative to using Eigenvalues we exploited the fact that the smallest eigenvalue is known to be real and used repeated bisection to find the appropriate zero of the characteristic equation of the matrix. We did not use the built-in function FindRoot as the very large gradients involved often seemed either to prevent convergence to the zero or to make it very slow. It turned out that the computations involved in doing this are numerically better behaved than those used in

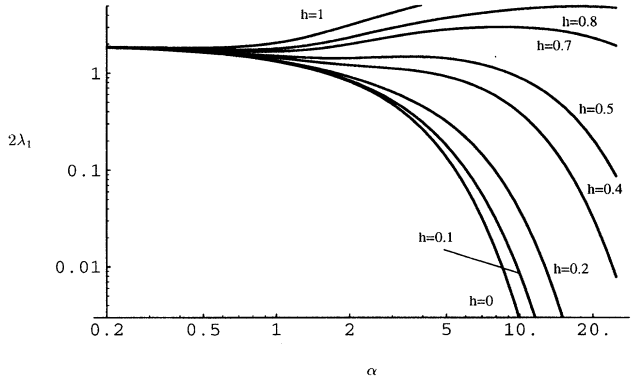

FIG. 3. The lowest nonvanishing eigenvalue λ_1 as a function of reduced barrier height α for $\psi=0$ that is the external field and easy axis are collinear (field parallel to the poles) (axially symmetric potential) for rotation of **M** in three dimensions for various values of reduced field h as computed from Eq. (14). The ordinate is shown as $2\lambda_1$ for easy comparison with the graphs of Ref. 20.

Eigenvalues and convergence was achieved with relative small matrices. For the purposes of drawing the graphs presented in Sec. VII, matrix sizes of 100×100 were sufficient for $\alpha\leqslant5$, 200×200 sufficed for $\alpha\leqslant10$, 400×400 for $\alpha\leqslant15$, and 600×600 for $\alpha\leqslant20$. Although this method of calculating the smallest eigenvalue was considerably slower than using Eigenvalues, it was faster than using Eigenvalues and working with 32 decimal places of precision (which also produces sensible results) by a factor of about 200. We did however use that method to provide an independent check of the accuracy of some of our calculations.

VII. RESULTS OF NUMERICAL COMPUTATION OF λ_1

We first discuss rotation when the external field and easy axis are collinear. The results shown in Figs. 3 and 4 for λ_1 as a function of α for $\psi=0$, with h as a parameter show that the qualitative behavior of λ_1 versus α is the same for both free and fixed axis rotation as has been shown analytically[3,8]

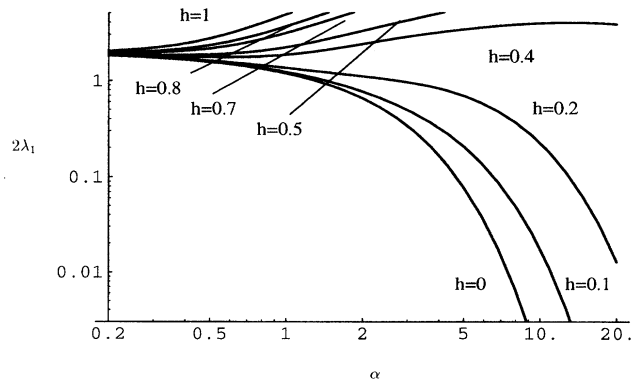

FIG. 4. As Fig. 3 supposing **M** rotates in a plane. Note the similar qualitative behavior of λ_1. The computations are carried out using Eq. (21).

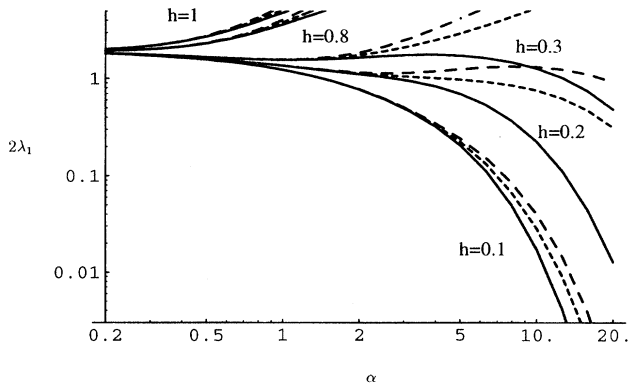

FIG. 5. Family of curves of λ_1 vs α for various values of h and ψ, for rotation in a plane as computed from Eq. (21): solid line $\psi=0$, small dashed line $\psi=\pi/8$, large dashed line $\psi=\pi/4$. Note the pronounced effect of the relative orientation of field and easy axis for $h>0.1$ and $\alpha>5$.

when $h=0$. Figure 5 shows the behavior of λ_1 as a function of α for $\psi=0$, $\pi/8$, and $\pi/4$, for various h values, demonstrating that the angular effect is very pronounced for large h and α. Figure 6 shows the behavior of λ_1 as a function of ψ for various h values, λ_1 passes through a maximum at $\psi=\pi/4$, corresponding to the smallest barrier height and returns to its $\psi=0$ value at $\psi=\pi/2$. Figures 7–14 represent the results of our investigation of rotation in space. In particular Figs. 6 and 8 exemplify the fundamental difference between fixed and free axis rotation, namely that $\lambda_1(\pi/2)<\lambda_1(0)$ so that the Néel relaxation time for large h and α is a maximum for the equatorial orientation of **H** while it is a minimum at the $\pi/4$ orientation. Such a result follows from the different boundary conditions which $W(\vartheta,\phi,t)$ and $F(\theta,t)$ must satisfy on account of the differences in the potentials for rotation in two and three dimensions. The effect is shown to an even more pronounced degree in Figs. 10–12 where $h=0.4$, 0.5, and 0.6, respectively, and values of α up to 20 are taken.

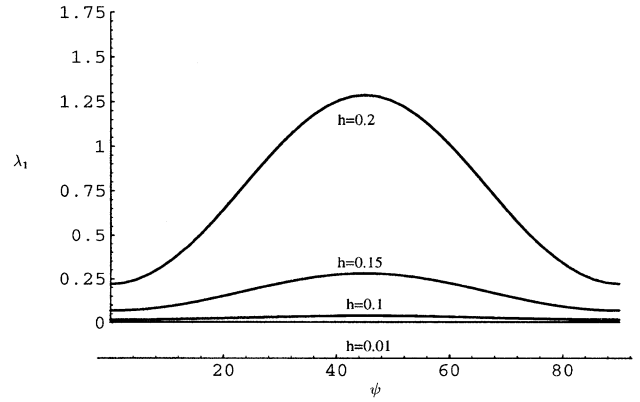

FIG. 6. λ_1 for rotation in a plane vs relative orientation ψ for various h values, note the maximum at $\psi=\pi/4$ corresponding to a minimum of the relaxation time for this orientation of the field. Curves computed from Eq. (21) for $\alpha=10$.

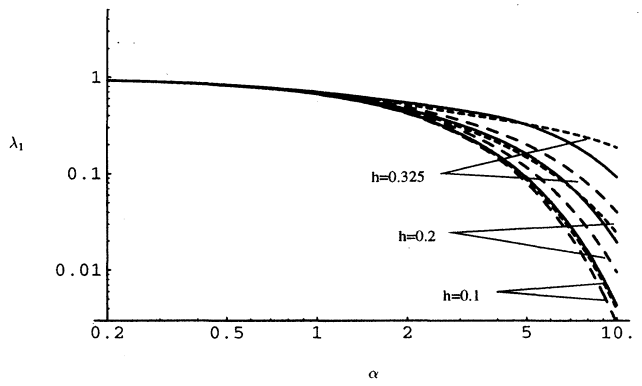

FIG. 7. Same as Fig. 5 but λ_1 as a function of α for various values of h and ψ for rotation in three dimensions computed from Eq. (14): solid line $\psi=0$ (axially symmetric potential, i.e., field parallel to the poles), small dashed line $\psi=\pi/4$, large dashed line $\psi=\pi/2$ field applied along the equator, family of curves 1, $h=0.325$, family of curves 2, $h=0.2$, family of curves 3, $h=0.1$.

In particular, there is a very large difference in λ_1 for the $\pi/2$ and $\pi/4$ orientations for $h\geq 0.5$ reflecting the fact that the two minima structure of the potential has vanished for $\psi=\pi/4$ when $h=0.5$. Figure 13 presents a comparison of the approximate formula for $\lambda_1(\pi/2)$ obtained by applying Eq. (72) to the $\pi/2$ orientation with the numerical solution. The approximate formula for $\lambda_1(\pi/2)$ is obtained as follows.

Since the potential for $\psi=\pi/2$ is a symmetric bistable one we have in Eqs. (68)–(71)

$$\nu_{12}=\nu_{21}, \tag{79}$$

$$I_1=I_2=he^{-\alpha h^2}\sqrt{\frac{\pi}{\alpha(1-h^2)}}, \tag{80}$$

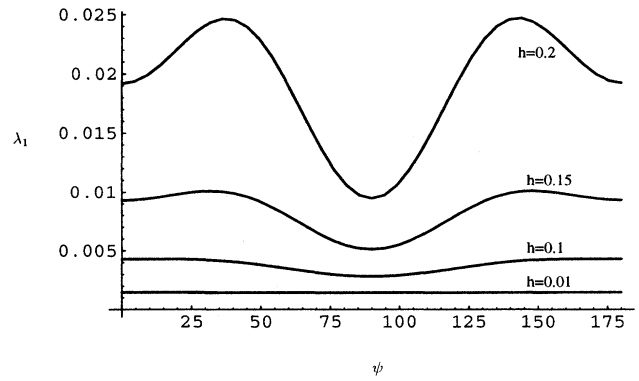

FIG. 8. λ_1 as a function of relative orientation ψ for various values of h for rotation of **M** in three dimensions: note the two unequal minima at $\psi=0$, $\pi/2$ and one maximum at $\psi=45°$. $\alpha=10$ in each case. Thus the Néel relaxation time is an absolute maximum when the field is applied along the equator $\psi=\pi/2$ and a minimum at the $\pi/4$ relative orientation. Note the differences in the maxima for the equatorial and polar orientations of the field.

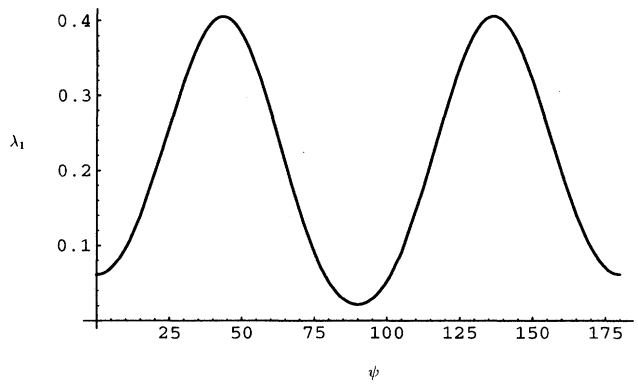

FIG. 9. Same as Fig. 8 however, λ_1 as a function of ψ for $\alpha=15$, $h=0.4$.

$$I_m=e^{\alpha(1-2h)}\sqrt{\frac{\pi}{\alpha(1-h)}}, \tag{81}$$

and so ($h\neq 0$)

$$\lambda_b=\lambda_1\cong\frac{\alpha(1-h)(1+h)^{1/2}e^{-\alpha(1-h)^2}}{\pi h}. \tag{82}$$

It appears by inspection of Fig. 13 that Eq. (82) appears to provide at least as good an approximation for $\alpha\geq 3$ and $h\geq 0.25$ (cf. Fig. 3 of Ref. 2) to the actual eigenvalue $\lambda_1(\pi/2)$ as the formula[2]

$$\lambda_1(0)\cong\pi^{-1/2}\alpha^{3/2}(1-h^2)(1-h)\exp[-\alpha(1-h)^2] \tag{83}$$

does to the actual $\lambda_1(0)$. The accuracy of Eq. (82) for small h values could possibly be improved by taking more terms in the method of steepest descents used to evaluate I_1, I_2, and I_m as in Ref. 3.

Explicit formulas for $\lambda_1(\psi)$ for other values of ψ may be given. Unfortunately, the various quantities in Eq. (72) usually become very cumbersome so it is best to evaluate that equation numerically. We illustrate by considering in detail the calculation for $\psi=\pi/4$ which proceeds as follows. We have from the condition for a stationary point namely

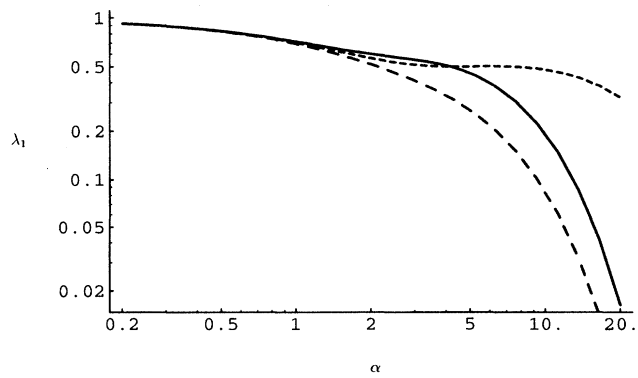

FIG. 10. λ_1 vs α for $h=0.4$, curves differentiated as in Fig. 7.

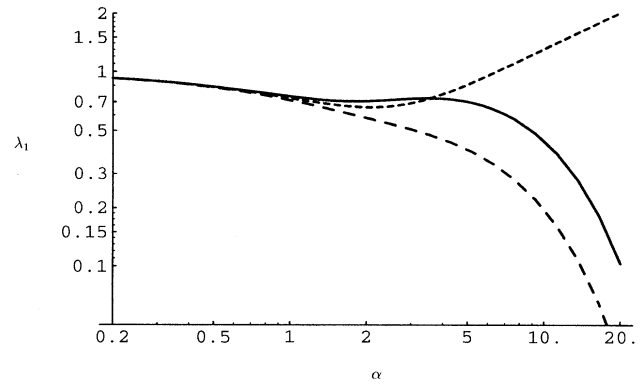

FIG. 11. Same as Fig. 10 but $h=0.5$. Note that the $\psi=\pi/4$ eigenvalue has lost its exponential character.

$$\sin 2\vartheta = -2h\ \sin(\vartheta-\psi) \tag{84}$$

with $s=\sin(\vartheta-\pi/4)$, $\psi=\pi/4$,

$$2s^2-2hs-1=0, \tag{85}$$

where we have utilized the fact that

$$\sin 2\vartheta = 1-2\ \sin^2\left(\vartheta-\frac{\pi}{4}\right). \tag{86}$$

The solution of Eq. (85) is

$$\sin\left(\vartheta-\frac{\pi}{4}\right)=\frac{h}{2}\pm\frac{\sqrt{h^2+2}}{2}. \tag{87}$$

We note that when $h=0$, $s_\pm=\pm\sqrt{2}/2$; as h increases, $-s_-$ decreases monotonically to a minimum value of 1/2 at $h=1/2$ while s_+ increases monotonically to a maximum value of 1 at $h=1/2$; thus

$$1/2\leqslant -s_-\leqslant\sqrt{2}/2\leqslant s_+\leqslant 1.$$

We also note that

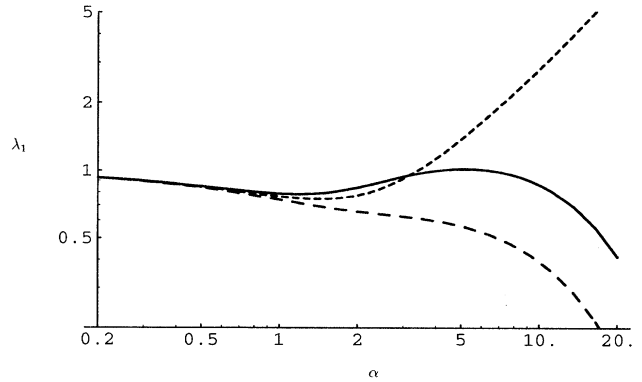

FIG. 12. Same as Fig. 11 but $h=0.6$. All computations in Figs. 7–12 are carried out using Eq. (14).

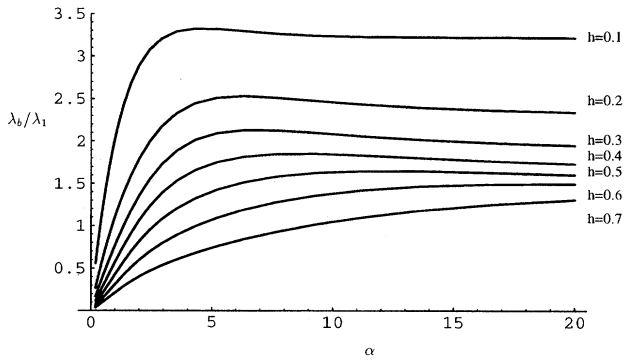

FIG. 13. Comparison of solution for $\lambda_1(\pi/2)$ yielded by the Kramers transition state method as applied to equatorial orientation of the field, i.e., Eq. (82) with exact solution computed from Eq. (14). All curves drawn for varying α with h as parameter.

$$\sin\left(\vartheta-\frac{\pi}{4}\right)=\sin\left[\pi-\left(\vartheta-\frac{\pi}{4}\right)\right]=\sin\left[\left(\frac{3\pi}{2}-\vartheta\right)-\frac{\pi}{4}\right], \tag{88}$$

hence if $\vartheta\geqslant\pi/4$ is a stationary point then so is $(3\pi/2-\vartheta)$. The three stationary points in the interval $(0,\pi)$ are thus

$$\vartheta_A=\frac{\pi}{4}-\sin^{-1}\left(-\frac{h}{2}+\frac{\sqrt{h^2+2}}{2}\right),\quad 0\leqslant\vartheta_A\leqslant\frac{\pi}{12},$$

$$\vartheta_m=\frac{\pi}{4}+\sin^{-1}\left(\frac{h}{2}+\frac{\sqrt{h^2+2}}{2}\right),\quad \frac{\pi}{2}\leqslant\vartheta_m\leqslant\frac{3\pi}{4},$$

$$\vartheta_B=\frac{5\pi}{4}-\sin^{-1}\left(\frac{h}{2}+\frac{\sqrt{h^2+2}}{2}\right),\quad \frac{3\pi}{4}\leqslant\vartheta_B\leqslant\pi. \tag{89}$$

At $h=0$, $\vartheta_A=0$, $\vartheta_m=\pi/2$, and $\vartheta_B=\pi$. As h increases ϑ_A increases monotonically to a maximum value of $\pi/12$ at $h=1/2(=h_c)$, ϑ_m increases monotonically to a maximum value of $3\pi/4$ at $h=1/2$, and ϑ_B decreases monotonically to a minimum value of $3\pi/4$ at $h=1/2$. We observe that at $h=1/2$, $\vartheta_m=\vartheta_B=3\pi/4$, we have a point of inflection. We have

$$\frac{\beta V''}{\alpha}=U''=2\ \cos 2\vartheta+2h\ \cos(\vartheta-\pi/4)$$
$$=\pm 2\sqrt{1-4h^2s^2}\pm 2h\sqrt{1-s^2}, \tag{90}$$

where the choice of sign depends on the quadrant in which the angle is located, hence

$$U''(\vartheta_A)=2\sqrt{1-4h^2s_-^2}+2h\sqrt{1-s_-^2}$$
$$=2\sqrt{1-2h^2(h^2+1)+2h^3(h^2+2)^{1/2}}$$
$$+h\sqrt{2}\sqrt{1-h^2+h(h^2+2)^{1/2}},\quad >0, \tag{91}$$

$$U''(\vartheta_B)=-U''(\vartheta_m)$$
$$=2\sqrt{1-4h^2s_+^2}+2h\sqrt{1-s_+^2}$$
$$=2\sqrt{1-2h^2(h^2+1)-2h^3(h^2+2)^{1/2}}$$
$$+h\sqrt{2}\sqrt{1-h^2-h(h^2+2)^{1/2}},\quad >0. \tag{92}$$

We observe that all the above quantities are positive, confirming that U has local minima at ϑ_A and ϑ_B and a local maximum at ϑ_m. To find $\sin\vartheta_A$,

$$2\sin\vartheta_A/\sqrt{2}=2\sin[\pi/4-\sin^{-1}(-s_-)]/\sqrt{2}$$
$$=s_-+\cos[\sin^{-1}(-s_-)].$$

Subtracting s_- and squaring gives

$$2\sin^2\vartheta_A-\frac{4s_-\sin\vartheta_A}{\sqrt{2}}+s_-^2$$
$$=\cos^2[\sin^{-1}(-s_-)]$$
$$=1-\sin^2[\sin^{-1}(-s_-)]=1-s_-^2,$$

which is a quadratic in $\sin\vartheta_A$,

$$2\sin^2\vartheta_A-\frac{4s_-}{\sqrt{2}}\sin\vartheta_A+2s_-^2-1=0.$$

Solving for $\sin\vartheta_A$, we obtain

$$\sin\vartheta_A=\frac{s_-\pm\sqrt{1-s_-^2}}{\sqrt{2}}.$$

Since $\sin\vartheta_A\geq 0$ and $s_-<0$ the correct root is given by

$$\sin\vartheta_A=\frac{s_-+\sqrt{1-s_-^2}}{\sqrt{2}}.$$

This quantity is however of interest in that it appears only in the $\nu_{1,2}$ term of λ_1 which gives the contribution due to the relatively small current of particles moving from the deep potential well at ϑ_A to the shallow potential well at ϑ_B. $\sin\vartheta_m$ is found in a similar way:

$$2\sin\vartheta_m/\sqrt{2}=2\sin[\pi/4+\sin^{-1}(s_+)]/\sqrt{2}$$
$$=s_++\cos[\sin^{-1}(s_+)].$$

Subtracting s_+ and squaring gives

$$2\sin^2\vartheta_m-\frac{2s_+\sin\vartheta_m}{\sqrt{2}}+s_+^2$$
$$=\cos^2[\sin^{-1}(s_+)]$$
$$=1-\sin^2[\sin^{-1}(s_+)]=1-s_+^2 \qquad (93)$$

which is a quadratic in $\sin\vartheta_m$,

$$2\sin^2\vartheta_m-\frac{4s_+}{\sqrt{2}}\sin\vartheta_m+2s_+^2-1=0. \qquad (94)$$

Solving for $\sin\vartheta_m$, we obtain

$$\sin\vartheta_m=\frac{s_+\pm\sqrt{1-s_+^2}}{\sqrt{2}}. \qquad (95)$$

To determine the correct root, we use the bounds $\pi/2\leq\vartheta_m\leq 3\pi/4$, hence $\sqrt{2}/2\leq\sin\vartheta_m\leq 1$; $\sqrt{2}/2\leq s_+\leq 1$ hence

$$0\leq\frac{s_+-\sqrt{1-s_+^2}}{\sqrt{2}}\leq\frac{\sqrt{2}}{2}\leq\frac{s_+\sqrt{1-s_+^2}}{\sqrt{2}}\leq 1. \qquad (96)$$

The correct root is therefore

$$\sin\vartheta_m=\frac{s_++\sqrt{1-s_+^2}}{\sqrt{2}}.$$

For $\sin\vartheta_B$, we have

$$2\sin\vartheta_B/\sqrt{2}=2\sin[5\pi/4-\sin^{-1}(s_+)]/\sqrt{2}$$
$$=s_+-\cos[\sin^{-1}(s_+)].$$

Subtracting s_+ and squaring gives

$$2\sin^2\vartheta_B-\frac{4s_+\sin\vartheta_B}{\sqrt{2}}+s_+^2$$
$$=\cos^2[\sin^{-1}(s_+)]$$
$$=1-\sin^2[\sin^{-1}(s_+)]=1-s_+^2$$

which is the quadratic in Eq. (93) and hence has roots given by Eq. (94). Since $3\pi/4\leq\vartheta_B\leq\pi$, $0\leq\sin\vartheta_B\leq\sqrt{2}/2$ and hence by Eq. (96)

$$\sin\vartheta_B=\frac{s_+-\sqrt{1-s_+^2}}{\sqrt{2}}.$$

The ratio $\sin\vartheta_m/\sin\vartheta_B$ is calculated as follows:

$$\sin\vartheta_B=\sin(3\pi/2-\vartheta_m)=-\cos\vartheta_m$$
$$=\sin 2\vartheta_m/2\ \sin\vartheta_m=\frac{\sqrt{2}hs_+}{s_++\sqrt{1-s_+^2}}$$

hence

$$\frac{\sin\vartheta_m}{\sin\vartheta_B}=\frac{(s_+\sqrt{1-s_+^2})^2}{2hs_+}=\frac{1+2s_+\sqrt{1-s_+^2}}{2hs_+}$$
$$=\frac{1}{h^2+h\sqrt{h^2+2}}+\frac{1}{h}\frac{(1-h^2-h\sqrt{h^2+2})^{1/2}}{\sqrt{2}}. \qquad (97)$$

The second barrier height is

$$B_2=\alpha(U_m-U_B)=\alpha\sin^2\vartheta_m-2h\alpha\cos(\vartheta_m-\pi/4)$$
$$-\alpha\sin^2\vartheta_B+2h\alpha\cos(\vartheta_B-\pi/4). \qquad (98)$$

Since $\vartheta_m-\pi/4$ is in the first quadrant

$$\cos(\vartheta_m-\pi/4)=\sqrt{1-\sin^2(\vartheta_m-\pi/4)}=\sqrt{1-s_+^2},$$

and since $\vartheta_B-\pi/4$ is in the second quadrant

$$\cos(\vartheta_B-\pi/4)=-\sqrt{1-\sin^2(\vartheta_B-\pi/4)}$$
$$=-\sqrt{1-\sin^2(\vartheta_m-\pi/4)}$$
$$=-\sqrt{1-s_+^2}.$$

Equation (98) becomes

$$B_2=2\alpha(s_+-2h)\sqrt{1-s_+^2}$$
$$=\alpha(-3h+\sqrt{h^2+2})\,\frac{(1-h^2-h\sqrt{h^2+2})^{1/2}}{\sqrt{2}}. \quad (99)$$

This is in agreement with Pfeiffer,[11] who has in addition obtained[12] the following simple approximation:

$$B_2\cong\alpha(1-2h)^{1.43}. \quad (100)$$

The higher energy barrier approximation is then

$$\lambda_1\cong\tau_N\nu_{2,1}\cong\alpha U''(\vartheta_m)e^{-B_2}\sin\vartheta_m/4\pi\sin\vartheta_B\cong\frac{\alpha(2\sqrt{1-4h^2s_+^2}+2h\sqrt{1-s_+^2})(1+2s_+\sqrt{1-s_+^2})}{8\pi hs_+}\exp[-\alpha(1-2h)^{1.43}]$$
$$=\frac{\alpha}{4\pi}(2\sqrt{1-2h^2(h^2+1)-2h^3(h^2+2)^{1/2}}+h\sqrt{2}\sqrt{1-h^2-h(h^2+2)^{1/2}})\left(\frac{1}{h^2+h\sqrt{h^2+2}}\right.$$
$$\left.+\frac{1}{h}\frac{(1-h^2-h\sqrt{h^2+2})^{1/2}}{\sqrt{2}}\right)\exp[-\alpha(1-2h)^{1.43}]. \quad (101)$$

The first barrier height B_1 is given by

$$B_1=\alpha(U_m-U_A)=\alpha\sin^2\vartheta_m-2h\alpha\cos(\vartheta_m-\pi/4)-\alpha\sin^2\vartheta_A+2h\alpha\cos(\vartheta_A-\pi/4)$$
$$=B_2/2+\alpha(2h-s_-)\sqrt{1-s_-^2}=\frac{B_2+\alpha(3h+\sqrt{h^2+2})}{2}\,\frac{(1-h^2+h\sqrt{h^2+2})^{1/2}}{\sqrt{2}}\cong\alpha(1-2h)^{1.43}+4\alpha h/\sqrt{2}. \quad (102)$$

Equation (101) is compared with the exact solution for $h=0.4$ and all values of α in Fig. 14. It is apparent that it provides a reasonable estimate of the exact λ_1 for $\alpha\geq 2$ and $h=0.4$. Once again the accuracy could be improved by taking more terms in the method of steepest descents and including ν_{12}.

VIII. DISCUSSION OF RESULTS AND CONCLUSIONS

We have discussed the problem of Néel relaxation in the presence of an applied field which is not coincident with the easy axis of magnetization by calculating the smallest nonvanishing eigenvalue λ_1 of the appropriate Fokker-Planck equation assuming that the field is applied along a line of longitude. The results for high barrier heights are in substantial agreement with those predicted by the Kramers transition state theory and demonstrate that the approximate formula for the barrier height as a function of relative orientation and magnitude of the reduced field [Eq. (42)] given by Pfeiffer[11,12] yields an adequate description of the behavior of the argument of the exponential factor in the exact solution. This suggests[17] that a valuable addition to the theory which would be of particular interest in the context of macroscopic quantum tunnelling of the magnetization[18] would be an analytical formula for $\lambda_1(\psi)$ for large potential barriers, that is an explicit evaluation of the various derivatives in Eq. (72). This may be accomplished using methods due to Geogheghan[19] for the solution of the equation for the stationary points.

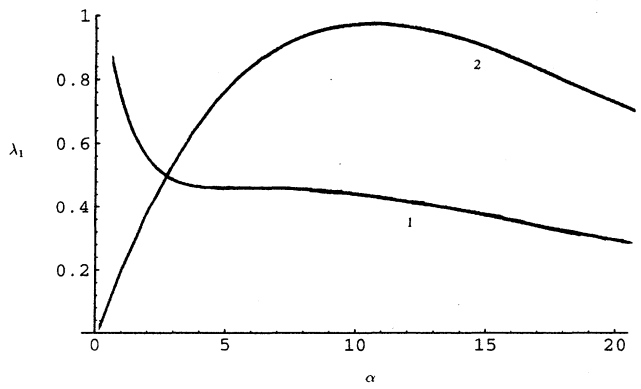

FIG. 14. Exact solution (curve 1) for $h=0.4$ and $\psi=\pi/4$ vs α compared with asymptotic estimate (curve 2) rendered by Eq. (101).

We remark that throughout this analysis we have assumed that the response is dominated by the mode characterized by λ_1. A complete analysis of the problem would require a knowledge of the decay of the magnetization which in turn requires one to calculate all the other eigenvalues and their associated amplitudes that is the complete aftereffect solution of the Fokker-Planck equation. This procedure allows one to ascertain the contribution of each decay mode to the overall decay. Such a calculation is important,[20] as in the presence of a field λ_1^{-1} differs markedly from the correlation time[20] (defined as the area under the curve of the decay of

the magnetization) due to the nonvanishing contribution of the other decay modes. The second assumption we have made is that the gyromagnetic terms in the Fokker-Planck equation may be ignored. The inclusion of these will always affect the behavior of λ_1.

For large barrier heights however,[16,19] they will affect only the prefactor of Eq. (72). The inclusion of these terms gives rise to extra terms in the differential-recurrence relation of the form

$$\frac{\xi\cos\psi}{2l+1}\left\{-\frac{im(2l+1)}{a}c_{l,m}\right\}+\frac{\xi\sin\psi}{2(2l+1)}\left\{\frac{i(2l+1)(l+m)(l-m+1)}{a}c_{l,m-1}+\frac{i(2l+1)}{a}c_{l,m+1}\right\}+2\alpha\left\{-\frac{im}{a}\frac{l+m}{2l+1}c_{l-1,m}-\frac{im}{a}\frac{(l-m+1)}{2l+1}c_{l+1,m}\right\},$$

where the decay modes c_{lm} are now of the form

$$\langle P_l^m(\cos\vartheta)e^{im\phi}\rangle-\langle P_l^m(\cos\vartheta)e^{im\phi}\rangle_0$$

since $\langle P_l^m(\cos\vartheta)\sin m\phi\rangle$ must now arise in the solution. The detailed derivation of the differential recurrence relation from the Fokker-Planck equation which requires intricate manipulation of the recurrence relations for the spherical harmonics $Y_{l,m}(\vartheta,\phi)$ is given by Coffey and Geoghegan in Ref. 21 and by Kalmykov in Ref. 22 who has shown how the recurrence relations for the $c_{l,m}$ may be derived directly[23] from the Gilbert-Langevin equation[16] describing the rotation of **M**.

We remark in conclusion that the numerical difficulties associated with the oblique field problem arise because the lack of axial symmetry increases the number of equations to be solved in the matrix equation

$$\dot{\mathbf{X}}=\mathbf{AX}$$

by a factor of $(L+3)/2$ where $1\leqslant l\leqslant L$ thus introducing the loss of precision in floating point calculations which has so bedevilled nonaxially symmetric problems.[14–16] An accurate calculation in such cases will always require one to resort to a very fast computer such as the CRAY.[24]

ACKNOWLEDGMENTS

We thank the British Council and the FORBAIRT/CNRS exchange scheme for financial support for this work. One of us, (Yu. P. Kalmykov) would like to thank the Royal Irish Academy for support. D.S.F.C. acknowledges UK-SERC Rolling Grant No. GR/K24741.

*Corresponding author.

[1] W. F. Brown, Jr., Phys. Rev. **130**, 1677 (1963).
[2] A. Aharoni, Phys. Rev. **170**, 793 (1969).
[3] W. T. Coffey, D. S. F. Crothers, Yu. P. Kalmykov, E. S. Massawe, and J. T. Waldron, Phys. Rev. E **49**, 1869 (1994).
[4] H. A. Kramers, Physica **7**, 284 (1940).
[5] H. Risken, *The Fokker-Planck Equation* (Springer-Verlag, Berlin, 1984).
[6] P. Hänggi, P. Talkner, and M. Borkovec, Rev. Mod. Phys. **62**, 251 (1990).
[7] J. L. Dormann, in *Magnetic Properties of Fine Particles*, edited by J. L. Dormann and D. Fiorani, North-Holland Delta Series (North-Holland, Amsterdam, 1991), p. 115.
[8] W. T. Coffey, Yu. P. Kalmykov, E. S. Massawe, and J. T. Waldron, J. Chem. Phys. **99**, 4011 (1993).
[9] A. R. Edmonds, *Angular Momentum in Quantum Mechanics* (Princeton University Press, Princeton, NJ, 1957).
[10] J. L. Dormann, D. Fiorani, and M. El Yamani, Phys. Lett. A **120**, 95 (1987).
[11] H. Pfeiffer, Phys. Status Solidi **122**, 377 (1990).
[12] H. Pfeiffer, Phys. Status Solidi **118**, 295 (1990).
[13] E. C. Stoner and E. P. Wohlfahrt, Philos. Trans. R. Soc., London Ser A **240**, 599 (1948).
[14] I. Eisenstein and A. Aharoni, Phys. Rev. B **16**, 1279 (1977).
[15] I. Eisenstein and A. Aharoni, Phys. Rev. B **16**, 1285 (1977).
[16] W. F. Brown, Jr., IEEE Trans. Magn. Mag-15, 1197 (1979).
[17] R. W. Chantrell (private communication).
[18] E. M. Chudnovsky, J. Appl. Phys. **73**, 6697 (1993).
[19] L. J. Geogheghan, Ph.D. thesis, University of Dublin, 1995.
[20] W. T. Coffey, D. S. F. Crothers, Yu. P. Kalmykov, and J. T. Waldron, Phys. Rev. B **51**, 15947 (1995).
[21] W. T. Coffey and L. J. Geogheghan (unpublished).
[22] Yu. P. Kalmykov (unpublished).
[23] W. T. Coffey, J. Chem. Phys. **99**, 3014 (1993).
[24] A. W. Wickstead (private communication).